# Bose-Einstein Condensation in Solid $^4$He

S. O. Diallo,[1] J. V. Pearce,[2] R. T. Azuah,[3,4] O. Kirichek,[5] J. W. Taylor,[5] and H. R. Glyde[1]

[1]*Department of Physics and Astronomy, University of Delaware, Newark, Delaware 19716-2593, USA*
[2]*National Physical Laboratory, Teddington, United Kingdom*
[3]*NIST Center for Neutron Research, Gaithersburg, Maryland 20899-8562, USA*
[4]*Department of Materials Science and Engineering, University of Maryland, College Park, Maryland 20742-2115, USA*
[5]*ISIS Spallation Neutron Source, Rutherford Appleton Laboratory, Chilton, Didcot, OX11 0QX, United Kingdom*

(Received 14 February 2007; published 17 May 2007)

We present neutron scattering measurements of the atomic momentum distribution $n(\mathbf{k})$ in solid helium under a pressure $p = 41$ bar (molar volume $V_m = 20.01 \pm 0.02$ cm$^3$/mol) and at temperatures between 80 and 500 mK. The aim is to determine whether there is Bose-Einstein condensation (BEC) below the critical temperature, $T_c = 200$ mK, where a superfluid density has been observed. Assuming BEC appears as a macroscopic occupation of the $k = 0$ state below $T_c$, we find a condensate fraction of $n_0 = (-0.10 \pm 1.20)\%$ at $T = 80$ mK and $n_0 = (0.08 \pm 0.78)\%$ at $T = 120$ mK, consistent with zero. The shape of $n(\mathbf{k})$ also does not change on crossing $T_c$ within measurement precision.

DOI: 10.1103/PhysRevLett.98.205301 PACS numbers: 67.80.−s, 61.12.Ex, 67.90.+z

In 2004, Kim and Chan [1,2] reported the spectacular observation of a superfluid density in solid helium below a critical temperature $T_c$. The superfluid density $\rho_S$ is observed as a nonclassical rotational inertia (NCRI) in a torsional oscillator (TO) containing solid helium. The percent of solid that has a NCRI and is decoupled from the rest of the solid was $\rho_S(T) \simeq 1.5\%$ at temperature $T = 50$ mK in commercial grade purity $^4$He which contains typically 0.3 ppm of $^3$He, where $T_c = 200$ mK. All other impurities are frozen out. A $\rho_S$ was observed in both bulk solid helium [2] and in solid confined in porous media (Vycor) [1]. The magnitude of $\rho_S$ varies somewhat from solid sample to solid sample [3]. A superfluid density was observed in solids at pressures between $p \sim 25$ bar near the melting line and 135 bar with $\rho_S$ taking its maximum value of 1.5% at $p \sim 50$ bar.

This remarkable result has been confirmed in independent TO measurements [4–6]. Rittner and Reppy [5] find that $\rho_S$ can be significantly reduced by annealing the solids near their melting temperatures with $\rho_S$ reduced to zero in some cases. Similarly, Shirahama *et al.* [4] report a reduction in $\rho_S$ of up to 50% by annealing. Macroscopic superflow was not observed in helium in Vycor [7] and bulk helium [8]. However, Sasaki *et al.* [9] have observed macroscopic superflow in those solids which contain grain boundaries that extend across the solid. This unexpected result suggests that there is indeed superflow and that it is along or associated with grain boundaries. Superflow related to grain boundaries [9], the variation of $\rho_S$ from sample to sample [3], and the reduction of $\rho_S$ by annealing [4,5] suggest that a superfluid density may be associated with macroscopic defects that extend across or whose impact extends across the whole solid.

In liquid helium, Bose-Einstein condensation (BEC) and superfluidity are observed together. Indeed superflow can be shown to follow from BEC [10,11]. It can also be shown to arise from long range atomic exchanges [12]. In the liquid, both in bulk [13] and in Vycor [14], BEC is observed as a macroscopic occupation of the $k = 0$ state in $n(\mathbf{k})$, as expected for a translationally invariant system. For certain models of superflow in solid helium, such as a gas of vacancies, we anticipate that BEC will appear as a macroscopic occupation of $k = 0$ in $n(\mathbf{k})$. In this context we look for an enhancement of $n(\mathbf{k})$ at $k \sim 0$ below $T_c$. We also look for a change in shape of $n(\mathbf{k})$ below $T_c$. The central result is that we observe no increase in $n(\mathbf{k})$ at $k \sim 0$ nor any change in shape of $n(\mathbf{k})$ as the temperature is lowered below $T_c$.

In 1969, Andreev and Lifshitz [15] proposed that helium could be a supersolid if the solid contained vacant sites in the ground state. Essentially, the ground state, zero point vacancies could form a Bose gas at $T \sim 0$ K in which the Bose-Einstein condensate fraction $n_0$ and $\rho_S$ are both approximately 100%. While thermally activated vacancies have been observed [16], ground state vacancies have not. Chester [17] proposed that superflow in solid helium may be possible because the solid is well described by fluidlike wave functions that support superflow. Leggett [18] examined superflow via long range exchanges of atoms within a perfect helium solid and found superflow possible but that $\rho_S$ would be small, $\rho_S \sim 0.01\%$.

Recent accurate path integral Monte Carlo calculations [19] find that $\rho_S$ arising from long range atomic exchanges in a perfect crystal will be unobservably small. Similarly, BEC in bulk perfect crystals is predicted to be very small [20,21], $n_0 \leq 10^{-8}$. Zero point vacancies in the ground state are predicted to be unstable [22]. Essentially, vacancies migrate to a surface or coalesce to create a surface and leave the crystal. However, if solid helium is held in an amorphous rather than the equilibrium crystal state, both $\rho_s$ and $n_0$ take significant values [20], e.g., $n_0 = 0.5\%$, $\rho_S = 10\%$–$60\%$ depending upon density. With these predictions, it is interesting to search for BEC where $\rho_S$ is observed.

 

The solid $^4$He investigated in this experiment was grown using the blocked capillary method. Commercial grade purity $^4$He (0.3 ppm $^3$He) was introduced into a cylindrical Al sample cell of 20 mm diameter and 62 mm height at a temperature $T \simeq 3$ K to a pressure of $p \simeq 70$ bar. At constant $p$, the temperature was reduced using an Oxford Instruments Kelvinox VT dilution refrigerator until solid formed in the capillary and blocked the cell. The block was observed at filling $p = 69.8 \pm 0.2$ bar and $T = 2.79 \pm 0.02$ K, which corresponds to liquid on the melting line at a molar volume $V_m = 20.01 \pm 0.02$ cm$^3$/mol [23]. The blocked cell was further cooled and neutron inelastic scattering measurements at high momentum transfer were made in the solid hcp phase at 80, 120, 300, and 500 mK on the MARI spectrometer at the ISIS neutron facility.

Single atom dynamics is observed in the dynamic structure factor $S(Q, \omega)$ at high momentum transfer $\hbar Q$. Specifically, at $\hbar Q \rightarrow \infty$, where the impulse approximation (IA) is valid, the energy transfer $\hbar\omega$ in $S(Q, \omega)$ is Doppler broadened by the atomic momentum distribution $n(\mathbf{k})$. In this limit, it is convenient to express $\omega$ in terms of the "$y$ scaling" wave vector variable, $y = (\omega - \omega_R)/v_R$ where $\omega_R = \hbar Q^2/2m$ and $v_R = \hbar Q/m$, and to present the neutron inelastic data as $J(Q, y) = v_R S(Q, \omega)$. Including final state (FS) effects, which are small but not negligible at the $Q$ values investigated here, as a convolution denoted convolution approach (CA), we have

$$J(Q, y) = \int dy' R(Q, y - y') J_{\mathrm{IA}}(y'), \tag{1}$$

where $R(Q, y)$ is the FS broadening function and

$$J_{\mathrm{IA}}(y) = \int d\mathbf{k}\, n(\mathbf{k}) \delta(k_Q - y) = n_Q(y) \tag{2}$$

is the IA to $J(Q, y)$. Specifically, $J_{\mathrm{IA}}(y)$ is $n(\mathbf{k})$ projected along $\mathbf{Q}$ denoted the longitudinal momentum distribution [24].

Figure 1 shows the observed $J(Q, y)$ at wave vectors $Q = 26$ Å$^{-1}$ and temperatures $T = 120$ mK and $T = 300$ mK. The observed $J(Q, y)$ includes the MARI instrument resolution function which is shown separately as a dotted line in Fig. 1. The solid line is a fit of a model to the data as described below. We were able to determine at most two free parameters in model fits to the data.

To obtain a condensate fraction, we assumed a model $n(\mathbf{k})$ of the form

$$n(\mathbf{k}) = n_0 \delta(\mathbf{k}) + (1 - n_0) n^*(\mathbf{k}), \tag{3}$$

where $n^*(\mathbf{k})$ is the momentum distribution of the atoms above the condensate in the $k > 0$ states. To proceed, we assume (1) that the shape of $n(\mathbf{k})$ is the same as observed previously in solid helium at a somewhat lower pressure [25] and (2) that the FS function $R(Q, y)$ in Eq. (1) is the same as observed [13] in liquid helium. The free parameters (two) in the model are then $n_0$ and the width $\bar{\alpha}_2$ of the

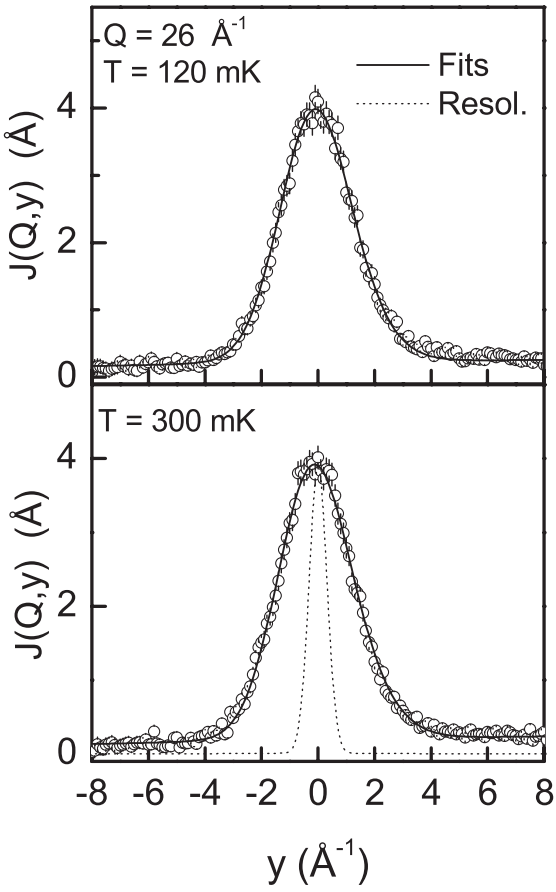


FIG. 1. Observed $J(Q, y)$ of solid $^4$He at $V_m = 20.01$ cm$^3$/mol (open circles) folded with the instrument resolution at momentum transfer $Q = 26$ Å$^{-1}$ and temperatures $T = 120$ (top) and 300 mK (bottom). The solid lines are fits of the convolution approach (CA) with final state (FS) function taken from liquid $^4$He (Ref. [13]), shape of $n(\mathbf{k})$ from Ref. [25], and width $\bar{\alpha}_2$ parameter as the single free fitting parameter. The data peaks below $y = 0$ because of FS effects. The dotted line is the MARI instrument resolution function.

Gaussian component of $n^*(\mathbf{k})$. A condensate component appears as an additional intensity unbroadened by $n^*(\mathbf{k})$ in $J_{\mathrm{IA}}(y)$ at $y = 0$.

We first fit the model $n(\mathbf{k})$ to the data at 500, 300, 120, and 80 mK assuming $n_0 = 0$ at all temperatures. The $n_0$ is expected to be zero at 300 and 500 mK. The resulting values of $\bar{\alpha}_2$, shown in Fig. 2, remain the same or perhaps decrease slightly with decreasing temperature. In a recent measurement, Adams *et al.* [26] find an $\bar{\alpha}_2$ independent of temperature within precision.

If superflow is associated with defects in the solid such as vacancies, we anticipate that BEC is similarly associated with these defects, perhaps in a vacancy gas. In this event, the parameter $\bar{\alpha}_2$ which sets the atomic kinetic energy may be largely unaffected by the BEC in the defects. To obtain $n_0$ at 80 and 120 mK within this picture we kept $\bar{\alpha}_2$ fixed at the values obtained above and refitted the model of Eq. (3) with $n_0$ as a free parameter. The fitted values of $n_0$ are

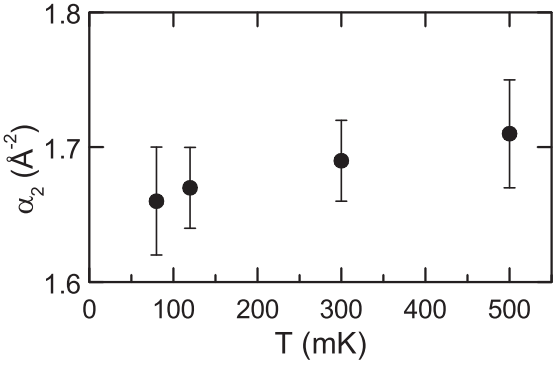


FIG. 2. The mean square atomic momentum $\bar{\alpha}_2 = \langle k_Q^2 \rangle$ along an axis of solid helium at $V_m = 20.01$ cm$^3$/mol versus temperature obtained from fits to $J(Q, y)$ such as shown in Fig. 4.

shown in Fig. 3. The variation of $n_0$ with $Q$ reflects the statistical error in $n_0$. The mean values are $n_0 = (-0.1 \pm 1.2)\%$ at 80 mK and $n_0 = (0.08 \pm 0.78)\%$ at 120 mK.

If, in contrast, the superflow and BEC lie within the bulk of the solid, we anticipate, as in liquid $^4$He, that the parameter $\bar{\alpha}_2$ will decrease below $T_c$ as a result of BEC. The observed decrease in $\bar{\alpha}_2$ below $T_c$ has been used to estimate $n_0$ in liquid $^4$He [27,28]. To address this case, we kept $\bar{\alpha}_2$ constant at the value obtained at 300 mK and refitted the model of Eq. (3) at 80 and 120 mK to obtain $n_0$. The resulting values are $n_0 = (0.8 \pm 1.2)\%$ at 80 mK and $n_0 = (0.76 \pm 0.77)\%$ at 120 mK. This method assumes that all the apparent drop in $\bar{\alpha}_2$ below $T_c = 200$ mK arises from BEC and gives an upper limit to $n_0$, still consistent with zero. For example, if we keep the $\bar{\alpha}_2$ fixed at its 500 mK value and refitted the model to determine $n_0$ at 300 mK we obtain $n_0 = (0.63 \pm 0.77)\%$. Since $n_0$ at 300 mK is zero, we expect the $n_0$ values below $T_c$ to be overestimated by approximately 0.6%. If we try to determine both $\bar{\alpha}_2$ and $n_0$ simultaneously, we get essentially the same values as before, with only larger error bars; e.g., $n_0 = (0.74 \pm 1.01)\%$ at $T = 120$ mK. Thus all methods give similar values of $n_0$.

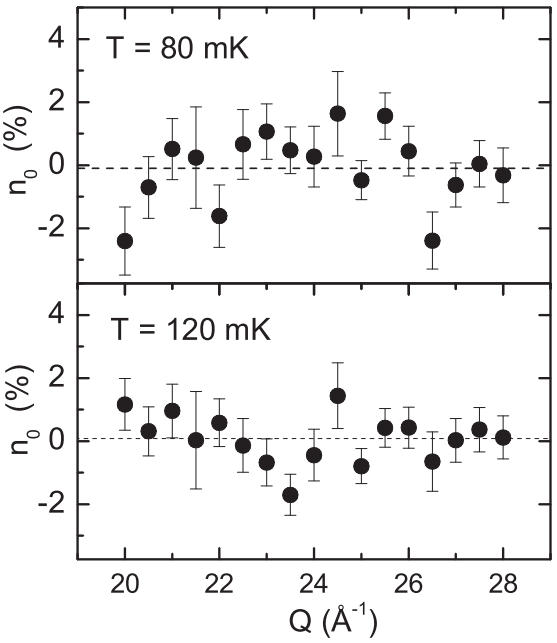


FIG. 3. Condensate fractions obtained by fitting the CA at $T = 80$ and 120 mK with the width of $n(\mathbf{k})(\bar{\alpha}_2)$ held fixed at its values shown in Fig. 2. We find $n_0 = (-0.10 \pm 1.20)\%$ at $T = 80$ mK and $n_0 = (0.08 \pm 0.78)\%$.

To investigate a possible change in shape of $J(Q, y)$ or $n(\mathbf{k})$ on crossing $T_c = 200$ mK, we fit the additive approach (AA) [29] to the data. In this model to lowest order, $J(Q, y)$ is [14,29]

$$J(Q, y) = \left[1 - \frac{\bar{\mu}_3}{2\bar{\alpha}_2^{3/2}}\left(x - \frac{x^3}{3}\right) + \frac{\bar{\mu}_4}{8\bar{\alpha}_2^2}\left(1 - 2x^2 + \frac{x^4}{3}\right)\right] J_G(x), \quad (4)$$

where $J_G = (1/\sqrt{2\pi\bar{\alpha}_2}) \exp(-x^2/2)$ and $x = y/\bar{\alpha}_2^{1/2}$. The second term in Eq. (4) is the leading FS term and the third term is the leading correction to a Gaussian $n(\mathbf{k})$ plus a FS term. The fitting parameters are $\bar{\alpha}_2$, $\bar{\mu}_3 = \bar{a}_3/\lambda Q$, and $\bar{\mu}_4 = \bar{\alpha}_4 + \bar{a}_4/(\lambda Q)^2$. Previously we found $\bar{a}_4 = 0$ [13,14,24]. The three remaining parameters are $\bar{\alpha}_2$, $\bar{\mu}_3$, and $\bar{\alpha}_4$. The kurtosis of $n(\mathbf{k})$ is $\delta = \bar{\alpha}_4/\bar{\alpha}_2^2$.

Figure 4 compares AA and simple Gaussian fits to data. The AA gives a better fit with the peak position lying at $y < 0$ in agreement with the data. We were able to determine only two parameters, e.g., $\hbar^2\mu_2 = (\lambda Q)^2\bar{\alpha}_2$ and $\hbar^3\mu_3 = (\lambda Q)^2\bar{a}_3$ where $\lambda = \hbar^2/m = 1.0443$ meV Å$^2$ = 12.12 K Å$^2$. These parameters are plotted in Fig. 5 and show the expected $Q$ dependence. We found again a smooth change in $\bar{\alpha}_2$ with temperature as shown in Fig. 2 and found $\bar{a}_3/\lambda$ independent of temperature. We tried keeping $\bar{\alpha}_2$ fixed and fitting for $\bar{\mu}_3$ and $\bar{\alpha}_4$, but we were

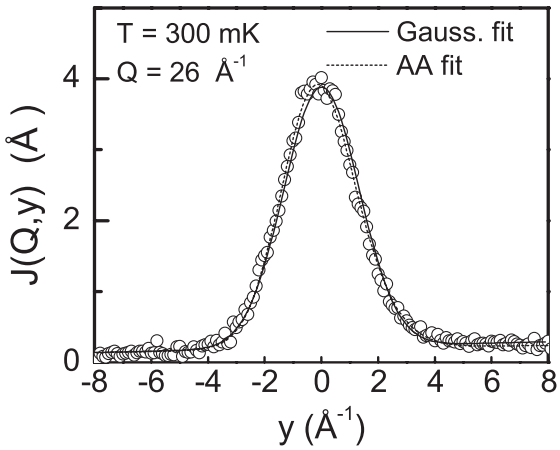


FIG. 4. Fits of the additive approach (AA ) which includes FS effects and a simple Gaussian to the observed $J(Q, y)$.

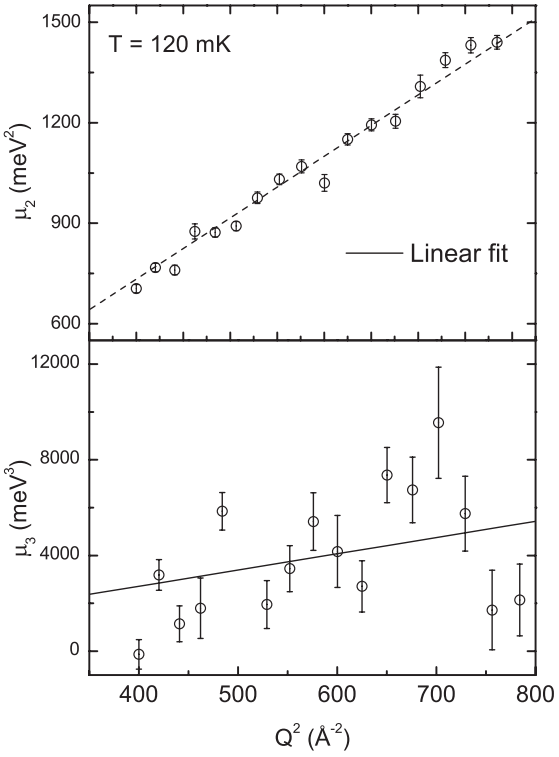


FIG. 5. Fitting parameters $\hbar^2\mu_2 = (\lambda Q)^2\bar{\alpha}_2$ and $\hbar^3\mu_3 = (\lambda Q)^2\bar{a}_3$ in the AA giving $\bar{\alpha}_2 = 1.67$ Å$^{-2}$ and $\bar{a}_3/\lambda = 6.21$ Å$^{-4}$.

not able to determine $\bar{\alpha}_4$. $\delta = 0$ or $\delta = 0.4$ fit equally well. Thus we find no change in the shape of $J(Q, y)$ or $n(\mathbf{k})$ at $T_c$ within precision.

To obtain the atomic kinetic energy $K$ we note that the observed $J(Q, y)$ does not come down to zero at high $y$ ($y > 4.0$ Å$^{-1}$) as it should (see Fig. 1). This may arise from multiple scattering contributions at high $y$. To obtain $K$ we removed the data for $y > 3.5$ Å$^{-1}$ and refitted to $J(Q, y)$. This leads to less precise $K$ values, e.g., $K = 25.6 \pm 1.0$ K at $T = 80$ mK and $K = 26.0 \pm 1.1$ K at $T = 500$ mK, but values which are unaffected by possible multiple scattering.

The condensate fraction $n_0$ of a perfect crystal is expected to be very small [20,21], $n_0 < 10^{-8}$, since BEC requires double occupation of a lattice site which has very high energy and is therefore very improbable. If there are vacant sites, $n_0$ in the crystal is dramatically increased, to $n_0 \simeq 0.23\%$ for a vacancy concentration $c_V \simeq 1\%$ [30]. If the solid is frozen in a nonequilibrium amorphous state, $n_0 \simeq 0.5\%$ [20]. The $n_0$ in the amorphous state is relatively insensitive to density although $\rho_S$ decreases significantly with increasing density [20]. The $n_0$ values within bulk solid helium including vacancies [30] or in extended amorphous regions [20], whether in equilibrium or not, are consistent with our observed value.

In summary, we have determined the BEC condensate fraction in commercial grade purity solid helium at pressure 41 bar and molar volume $V_m = 20.01$ cm$^3$/mol using inelastic neutron scattering. We find a condensate fraction $n_0 = (-0.10 \pm 1.20)\%$ at $T = 80$ mK below $T_c = 200$ mK consistent with zero. $T = 80$ mK is somewhat above but close to the temperature $T = 50$ mK at which $\rho_s$ reaches its maximum value [1,2]. We also find no change in the shape of the atomic momentum distribution on crossing $T_c$.

Support of this work by the U.S. DOE under Grant No. DE-FG02-03ER46038 and the ISIS facility is gratefully acknowledged.

[1] E. Kim and M. H. W. Chan, Nature (London) **427**, 225 (2004).
[2] E. Kim and M. H. W. Chan, Science **305**, 1941 (2004).
[3] E. Kim and M. H. W. Chan, Phys. Rev. Lett. **97**, 115302 (2006).
[4] K. Shirahama, M. Kondo, S. Takada, and Y. Shibayama, in *Proceedings of the American Physical Society March Meeting, Baltimore, 2006*, Abstract No. G41.00007 (unpublished).
[5] A. S. C. Rittner and J. D. Reppy, Phys. Rev. Lett. **97**, 165301 (2006).
[6] Adrian Choe, Science **311**, 1693 (2006).
[7] J. Day *et al.*, Phys. Rev. Lett. **95**, 035301 (2005).
[8] J. Day and J. Beamish, Phys. Rev. Lett. **96**, 105304 (2006).
[9] S. Sasaki *et al.*, Science **313**, 1098 (2006).
[10] P. Nozières and D. Pines, *The Theory of Quantum Liquids* (Perseus, Cambridge, MA, 1999).
[11] G. Baym, in *Mathematical Methods in Solid State and Superfluid Theory*, edited by R. C. Clark and G. H. Derrick (Oliver and Boyd, Edinburgh, 1969).
[12] D. M. Ceperley and E. L. Pollock, Phys. Rev. Lett. **56**, 351 (1986).
[13] H. R. Glyde *et al.*, Phys. Rev. B **62**, 14 337 (2000).
[14] R. T. Azuah *et al.*, J. Low Temp. Phys. **130**, 557 (2003).
[15] A. F. Andreev and I. M. Lifshitz, Sov. Phys. JETP **29**, 1107 (1969).
[16] R. O. Simmons, J. Phys. Chem. Solids **55**, 895 (1994).
[17] G. V. Chester, Phys. Rev. A **2**, 256 (1970).
[18] A. J. Leggett, Phys. Rev. Lett. **25**, 1543 (1970).
[19] D. M. Ceperley and B. Bermu, Phys. Rev. Lett. **93**, 155303 (2004).
[20] M. Boninsegni *et al.*, Phys. Rev. Lett. **96**, 105301 (2006).
[21] B. K. Clark and D. M. Ceperley, Phys. Rev. Lett. **96**, 105302 (2006).
[22] M. Boninsegni *et al.*, Phys. Rev. Lett. **97**, 080401 (2006).
[23] A. Driessen *et al.*, Phys. Rev. B **33**, 3269 (1986).
[24] *Momentum Distributions*, edited by R. N. Silver and P. E. Sokol (Plenum, New York, 1989).
[25] S. O. Diallo *et al.*, Phys. Rev. Lett. **93**, 075301 (2004).
[26] M. Adams *et al.*, Phys. Rev. Lett. **98**, 085301 (2007).
[27] V. F. Sears, Phys. Rev. B **28**, 5109 (1983).
[28] J. Mayers, C. Andreani, and D. Colognesi, J. Phys. Condens. Matter **9**, 10639 (1997).
[29] K. H. Andersen *et al.*, Phys. Rev. B **56**, 8978 (1997).
[30] D. E. Galli and L. Reatto, Phys. Rev. Lett. **96**, 165301 (2006).